Journal of Building Pathology and Rehabilitation (2024) 9:97
https://doi.org/10.1007/s41024-024-00452-0

RESEARCH ARTICLE

Sustainable use of steel slag as coarse aggregate and its influence on mechanical, durability properties, and microstructure of concrete

Saurabh Kalane[1] · Shubhangi Shekokar[1] · Sandeep Sathe[1] · Rohit Salgude[1]

Received: 1 April 2024 / Revised: 20 May 2024 / Accepted: 21 May 2024

Abstract
Construction materials are dealing with new challenges due to increased resource exploitation by globalized infrastructure. Research has consequently documented various waste management techniques that are focused on environmentally sustainable principles. The coarse steel slag aggregate (CSSA) can be reused as aggregate in cement concrete mixes. Hence, this experimental work considers an opportunity to investigate the effect of partial substitution of natural coarse aggregate (NCA) by CSSA for 20%, 40%, and 60% for the M40 grade concrete mix. The workability, mechanical, durability, and microstructural properties of concrete with CSSA were compared with NCA concrete on a 28-day curing. The 40% substitution of NCA by CSSA was found as the optimum ratio for the improvement in mechanical strength. Also, up to 20% of the substitution of CSSA satisfies the RCPT, water penetration, and acid attack (10% concentrated HCl acid) requirement given by standard codes.

Keywords Coarse steel slag aggregate · Natural coarse aggregate · Workability · Mechanical properties · Durability · Microstructural properties

1 Introduction

Ancient concrete use evolved into Roman innovations, paving the way for modern concrete construction dominance [1]. Modern concrete bends to the construction of buildings from homes to nuclear plants [2]. The flexibility of concrete design, environmental resilience, handling tough environments, and affordability make it a favorite for engineers. Concrete is unique from other construction materials in that it is made especially for civil engineering applications, and is primarily composed of cement, natural fine aggregates (NFA), natural coarse aggregate (NCA), water, etc. Almost 70% of the concrete volume is covered by NCA and has a huge requirement of 8 to 12 billion metric tons annually [3], which is increasing as per requirement and lead to a shortage of material resources in the future and cause environmental issues globally [4]. However, NCA holds the maximum volume of concrete which is made available from mining [5]. To address these environmental issues, the United Nations Framework Convention on Climate Change was held in December 2015 in Paris, emphasizing the requirement to save energy, reduce waste, and protect natural resources [6]. The researchers are researching for development of new materials with similar properties to NCA that can be used to replace them in concrete [7]. Sustainability can be significantly improved by utilizing waste materials that currently pollute our land. Researchers are actively exploring the use of industrial byproducts like slag, recycled construction debris, fly ash, and even waste glass and marble as substitutes in concrete [8–15].

However, the steel production industry is dynamic [16, 17], generating substantial sums of slag waste resulting from polluting lands by leaching heavy metals (chromium and lead) into the soil, which poses risks to plant growth and the ecosystem. This leaching of heavy metals can be reduced by utilizing steel slag waste as a substitute for the NCA in concrete [18, 19]. Steel slag is industrial waste that

✉ Saurabh Kalane
saurabhkalane015@gmail.com

✉ Shubhangi Shekokar
shubhangi.shekokar@mitwpu.edu.in

✉ Sandeep Sathe
sandeepsatheresearch@gmail.com

Rohit Salgude
rohit.salgude@mitwpu.edu.in

[1] Department of Civil Engineering, Dr. Vishwanath Karad MIT World Peace University, Pune, India

Published online: 30 May 2024

is generated during the manufacturing of steel [20], and around one ton of steel generates around 1300 to 2000 kg of steel slag waste [21]. Steel slag, an industrial waste from steel production, is recognized as a potential recycled raw material that contributes to a cleaner environment. This aligns with the ongoing efforts to address environmental concerns and promote sustainability in the construction and manufacturing industries.

In the past three decades, researchers have been investing in the utilization of steel slag for the substitution of NFA. Steel slag used as a substitute for NCA has particle sizes larger than 4.75 mm to meet the stability of NCA. Many researchers have experimented with the utilization of steel slag as a substitute for NCA in concrete mixes and also state that the substitution will enhance the mechanical properties of concrete [22–24]. Based on experimental results, [4, 16, 25, 26] observed that the 20% to 60% use of steel slag as aggregate in concrete gives similar strength results to that of conventional concrete, and [27] also states that up to 50% substitution by CSSA improved the mechanical strength for both M20 and M30 grades of concrete. Depending on the chemical properties, granulometry, mechanical, and physical properties, steel slag as aggregate has similar and considerable mechanical strength when compared with NCA. By reviewing past studies, Gencel et al. [28] stated that the CSSA above 50% and up to 100% of the substitutional ratio could be advantageous as a sustainable construction material without decreasing in strength. Mien et al. [29] that the use of CSSA could improve the chloride ion penetration and resistivity. The conclusion of the researchers on the past experimental study on the durability of CSSA is not the same. Researchers stated that the utilization of CSSA as NCA can hinder the entry of erosion ions and enhance the durability of concrete [30–33]. However, some researchers also state that the presence of free CaO in CSSA will lead to excessive expansion of concrete volume, which results in a decrease in the durability of the concrete [25, 34]. Moreover, the relevant experiments show that the free content of CaO in the well-weathered CSSA is low, which will have a low effect on the expansibility of CSSA [25] and also that the volume stability of concrete can be ignored only when the substitution rate of CSSA is less than 50% [35].

To improve the strength and stiffness of the concrete mixed with the steel slag, the substitution of natural aggregate can provide a sustainable solution to the environment and an alternative to natural aggregate in the future. This solution can also put an end to farmland problems, i.e., disposal of waste slag, and other environmental problems. Utilization of the waste steel slag in concrete can produce green concrete by contributing to energy savings and reducing the greenhouse emissions associated with natural aggregate extraction and processing.

2 Research significance

Based on the previous literature [30, 35, 36], studies have examined the problem associated with the use of natural aggregate in concrete and its impact on the environmental depletion of resources. There is also a gap in the literature regarding the use of CSSA (a sustainable alternative to NCA) in concrete, and its influence on concrete performance. This paper attempts to identify the aspects that influence the mechanical, durability, and microscopic properties of concrete by utilizing the CSSA, with a focus on the various percentages of CSSA as a substitution for NCA. The present study aims to establish an interrelation between CS, STS, and FS. The results of this paper are valuable because, utilizing CSSA as a substitute for NCA promotes sustainability by reducing reliance on finite resources, mitigating environmental impact associated with aggregate extraction, and repurposing industrial by-products, contributing to an eco-friendly construction industry.

3 Methodology

Through a comprehensive literature review, published research and articles, reports, and examining current global challenges related to the disposal of steel slag defined a clear and concise problem statement. As a sustainable solution, steel slag can be used as a partial substitution for NCA because of its properties and its utilization in concrete helps to reduce its disposal issue. For this objective, the performance of concrete with CSSA was analyzed in this research. This research investigates the effect of CSSA on the mechanical strength, durability, and microstructure of concrete. Various concrete mixes were designed, incorporating different percentages of NCA substituted with CSSA. After casting and curing the concrete specimens for 28 days, mechanical testing (CS, FS, STS) and durability testing (RCPT, water penetration, acid attack) were performed to assess the impact of CSSA content. Additionally, microstructure analysis using XRD and SEM techniques was performed to understand the internal changes in the concrete. By analyzing all the data, it was aimed to identify how CSSA influences the properties of concrete, exploring both its potential benefits and drawbacks as a partial substitute for NCA, this research contributes to the development of more sustainable and eco-friendly concrete. The methodology and experimental program followed by the Indian Standard Code as shown in Fig. 1.

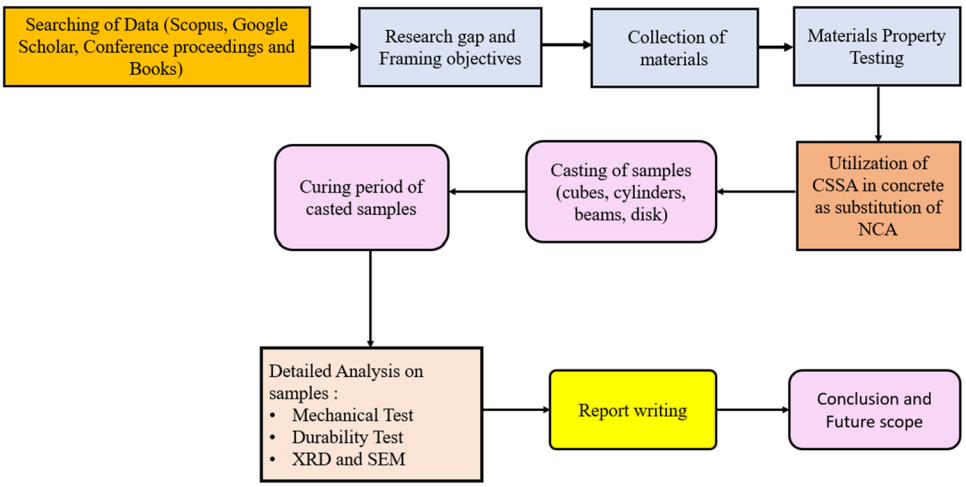

Fig. 1 Followed methodology of the experimental work

4 Materials properties

4.1 Materials

An experiment was performed as per the methodology shown in Fig. 1 to investigate the influence of CSSA as coarse aggregate on the properties of concrete. The materials used are cement, FA, NCA, CSSA, and water. The CSSA was collected and sieved to obtain in the range of 10 mm to 20 mm size for partial substitution of NCA.

4.1.1 Cement

Ordinary Portland cement (53 grade) was used and a test on OPC was performed as per IS4031-1996 [37]. The test performed and obtained properties are summarized in Table 1.

4.1.2 Fine aggregate (FA)

The FA was obtained from crushed stone and was used as FA in concrete. The crushed stone FA used in this experiment was passed through IS sieve no. 480 (4.75 mm), which falls in zone 3 as per IS383:2016 [39]. The properties of the FA are summarized in Table 2.

Table 1 OPC (53 grade) properties

Properties	Values	Limitations given by IS12269:2004 [38]
Specific gravity	3.13	≤3.15
Fineness	6%	< 10%
Consistency	30%	30%—35%
Initial setting time	40 min	> 30 min
Final setting time	205 min	< 600 min

4.1.3 Natural coarse aggregate (NCA)

The NCA used was nominal in size 10 mm–20 mm as per IS383:2016 [39]. Properties of NCA were compared to the CSSA used in this experimental work for the substitution of NCA as per IS383:2016 [39], as shown in Table 3, and the particle size gradation curve was obtained by sieve analysis which is shown in Fig. 2.

4.1.4 Steel slag aggregate (SSA)

The crushed SSA was collected from a blast furnace located in Chhattisgarh, India, as shown in Fig. 3a. The color profile observed of SSA is characterized by ranging from dark grey to black, with various complexities based on the chemical structure of the basic materials used to produce steel. The CSSA is granular, porous, and rough, as a result of the crystalline structure formed during the rapid cooling process of the molten steel. There is observable textural variation, with some samples having an even more glassy or vesicular texture. The variety of shapes that SSA can take on, including angular, rigid, and spherical ones, is a direct result of the complex processes involved in cooling and solidification. The texture of CSSA is shown in Fig. 3b.

Table 2 FA properties

Test conducted	FA	IS code
Specific gravity	2.61	IS 2720:1980-Part 3 [40]
Bulk density	1602 kg/m^3	IS 2386:1963-Part 3 [41]
Water absorption	0.6%	IS 2386:1963-Part 4 [42]
Fineness Modulus	3.3	IS 2386:1963-Part 5 [43]

Table 3 The properties of NCA and CSSA

Test conducted	NCA	CSSA	IS code
Specific gravity	2.71	3.44	IS 2386:1963-Part 3 [41]
Bulk density	1650 kg/m^3	1797 kg/m^3	IS 2386:1963-Part 3 [41]
Water absorption	0.81%	3.05%	IS 2386:1963-Part 3 [41]
Impact value	18.61%	9.44%	IS 2386:1963-Part 4 [42]
Crushing value	18.10%	20.83%	IS 2386:1963-Part 4 [42]
Loss Angeles (LA) abrasion	25.78%	13.46%	IS 2386:1983-Part 4 [42]

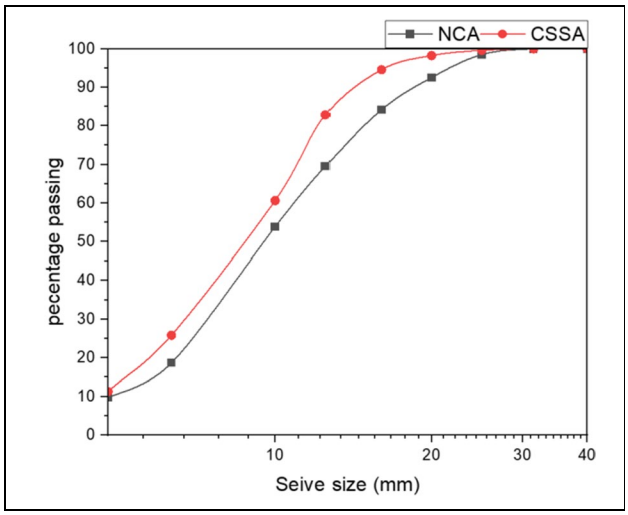

Fig. 2 Sieve analysis NCA and CSSA

The physical and chemical properties of NCA and CSSA are summarized in Table 3 respectively.

The chemical bonding in SSA/CSSA is also more complex, involving the production of oxides and minerals, with SiO_2, Al_2O_3, and CaO being important which is shown in Table 4.

To analyze the chemical composition of oxides, the XRD analysis of the SSA sample is compared with the oxides of cement as shown in Figs. 4 and 5. The XRD of SSA in Fig. 5 resulted at 2θ, has sharp crystalline peaks in a relatively broadband, and the same results were observed by M.H. Lai et al. [44]. Similar to cement, the SSA contains cementitious compounds like C_3S and C_2S. The presence of free MgO and CaO, which hydrate to form $Mg(OH)_2$ and $Ca(OH)_2$, negatively impacts the integrity of concrete mixtures. The free CaO has a more significant impact on stability than MgO because CaO hydrates much slower [45]. SSA is waste generated during the production of steel, it tends to react with water, air, or CO_2 to form the chemical products $Ca(OH)_2$ and $CaCO_3$. However, the reaction is slow, which limits the decrease of magnesium oxide (MgO) content. This allows for easier detection of free calcium oxide (CaO) in the SSA, ultimately enhancing its volume stability. Usually, the SSA is of the RO phase, which includes MgO, MnO, and FeO. These compounds are more stable than MgO and won't cause any unsoundness in the concrete mix. Figure 5 showed that most of the Mg minerals are in the form of $MgFe_2O_4$ content, which states that the MgO has precipitated from the RO-phase, which could react with the content of Fe_2O_3 and can also be transformed into $MgFe_2O_4$. The same observation was noticed by [46]. This results in overcome from the free content of MgO and CaO. To overcome the issue of unsoundness, the mixed concrete can be filled into the steel tube or also in the fiber-reinforced polymer tube, which results in improving the confining stress and the behavior of composite structures [44, 47–49].

Fig. 3 **a** Crushed SSA. **b** CSSA

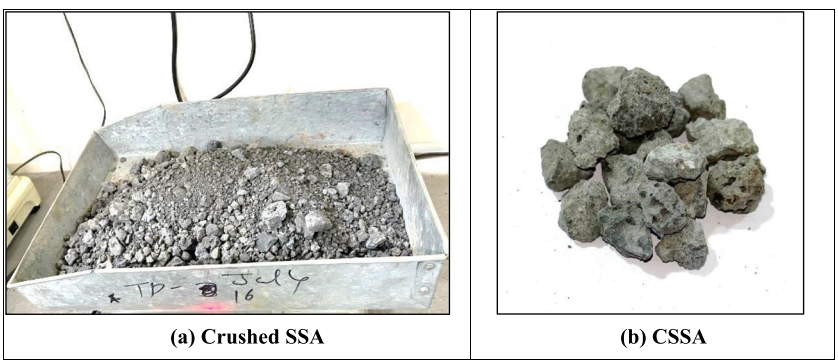

Table 4 Chemical properties of CSSA and cement

Oxides	CSSA	Cement
SiO_2	13.00%	18.96%
Al_2O_3	3.60%	4.19%
Fe_2O_3	32.00%	4.25%
CaO	40.00%	66.58%
MgO	7.00%	0.97%
Mn_2O_3	1.80%	-
TiO_2	0.33%	-
P_2O_3	0.45%	-
K_2O	0.14%	0.73%
Na_2O	0.16%	0.32%
SrO	0.03%	-
SO_3	0.86%	3.5%
Cl	0.02%	-
BaO	0.00%	-
Cr_2O_3	0.16%	-
V_2O_5	0.07%	-
Co_2O_5	0.06%	-

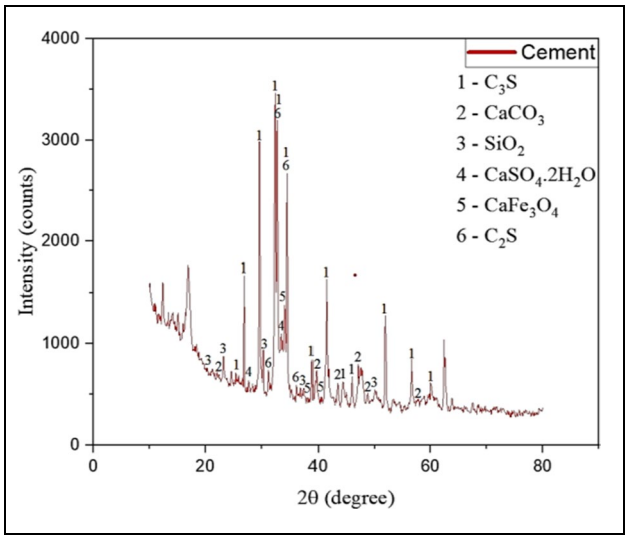

Fig. 4 XRD pattern of cement

5 Concrete mix design

The mix design was carried out as per IS10262:2019 [50]. Also, the design calculation was carried out based on water absorption, specific gravity, and free moisture content of the material i.e., cement, FA, NCA, CSSA, and water [3]. M40 grade of the concrete mix was designed with a mix proportion of 1: 1.99: 2.5 and w/c of 0.4. Table 5 shows the mix proportion for the substitution of CSSA by NCA at 0%, 20%, 40%, and 60%.

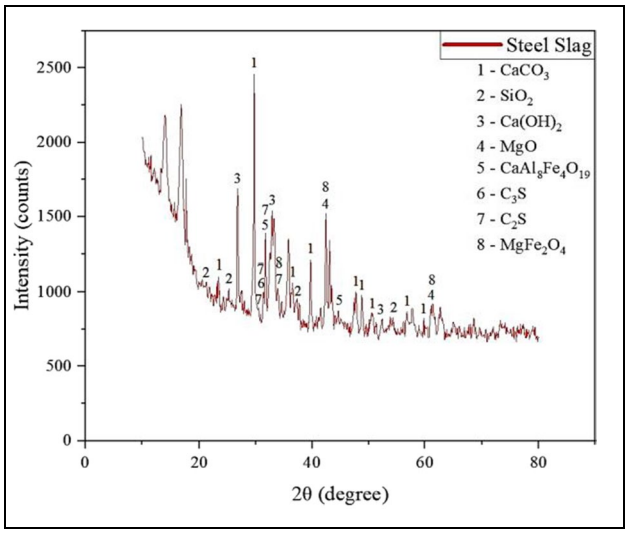

Fig. 5 XRD pattern of SSA

6 Experimental program

A rotating drum mixer was used to mix the material for the preparation of the concrete. All the materials were mixed as per IS10262:2019 [50], and the mix design ratio is shown in Table 5. A superplasticizer was used at the rate of 0.5% of cement and the w/c ratio was kept at 0.4 which was constant throughout the experiment to get a slump value within the range of 25-50 mm. The materials were first dry mixed for 1 min, then the lab tap water which was free from harmful elements was used for the mixing of concrete, and the mixing process continued for 2 min. After mixing, the slump test was performed as per IS1199:1959 [51] to check the water-cement (w/c) ratio and to get the required slump value, for the entire substitutional ratio of CSSA. Three samples were cast to assess the mix design percent substitution and were cured in the water as per IS10086:1982 [52].

6.1 Mechanical properties tests

6.1.1 Compressive strength test (CS)

The samples were made of cubes 150×150×150 mm in size as shown in Fig. 6. As per IS516:1959 [53], the 140 kg/cm^2/min of the load was applied for the compression on the cube sample till the failure in the compression machine for 7, 14, and 28 days of each 0%, 20%, 40%, and 60% substitution.

6.1.2 Split tensile strength test (STS)

The STS test was performed as per IS 5816:1999 [54], the cylinder samples were cast with a diameter of 150 mm and a height of 300 mm as shown in Fig. 7. In the STS test, the

Table 5 Mix proportion for the substitution (Kg/m^3)

Sample	Substitution (%)	Cement	FA	NCA	CSSA	Superplasticizer (%)
CSS0	0	443	881.57	1120.79	0	0.5
CSS20	20	443	881.57	896.63	224.16	0.5
CSS40	40	443	881.57	672.47	448.32	0.5
CSS60	60	443	881.57	448.32	672.47	0.5

Fig. 6 CS test of concrete on cube sample (150 × 150 x 150 mm)

Fig. 7 STS Test of concrete on cylinder sample (150 × 300 mm)

compressive line load of 1.2 N/mm^2 is applied along the opposing generators of a concrete cylinder with its axis horizontally positioned in between the patterns in the test method.

Fig. 8 FS test of concrete on beam sample (700 × 150 x 150 mm)

Fairly homogeneous tensile stress is created over roughly two-thirds of the loaded diameter as a result of the applied line loading. The specimen ultimately fails as a result of this tensile stress, splitting along the loaded diameter. For the STS test, 7- and 28-day results were noted for each substitution.

6.1.3 Flexural strength test (FS)

Since a direct tension test is a difficult method to evaluate the tensile strength of concrete, the tensile strength is calculated via a flexure test. So, for the FS test, the beam samples (150 × 150 × 700 mm) were cast and tested by following IS516:1959 [53]. The point load was applied to the beam sample at a load intensity of 140 kg/cm^2/min until failure as shown in Fig. 8. For the FS test, 7- and 28-day results were noted for each substitution.

6.2 Durability tests

6.2.1 Water penetration test

The water penetration test was conducted on the cube as per German code DIN1048 [55] for which the 3 samples per concrete cube were cast of 150 × 150 x 150 mm in size as shown in Fig. 9. The casted samples were curried for 28 days in the water. Dried cube, 3 of each sample are sealed

Fig. 9 Water penetration test (setup)

with wax and rosin. The test was carried out by the setup that consists of air compression connected to a water tank via a valve, and water pressure of 5N/mm^2 is applied to the concrete cube samples for 3 days (72 h). Using a system that consists of an air compressor connected to a water tank via a valve as shown in Fig. 9, water pressure is applied to the concrete cube in the form described in Eq. (1). Up to the point of reaching a steady state, the depth of water that percolates is recorded during the test period by illustrating the temperature at which the test is to be conducted, which is 27° ± 2° C. The depth of water penetration and the coefficient of permeability are shown in Table 7. The coefficient of permeability (K) was calculated by Eq. (1),

$$K = D^2P/2TH \quad (1)$$

where, D—Depth of penetration (mm), P—Porosity of concrete measured as a fraction, T—Time in seconds, H—Pressure head = 1.5 m.

6.2.2 Rapid chloride penetration test (RCPT)

RCPT was performed as per ASTM C1202 [56] to indicate the concrete resistance to the penetration for the passing of chloride ions and the samples were cast in the form of disks 100 mm in diameter and 50 mm in thickness. The test samples were placed between reservoirs holding 0.3% NaOH and 3% NaCl. The test sample was placed under a direct current of 60 V for approximately 6 h. The degree of the chloride ion penetration of the concrete was determined using ASTM C1012-04, and coulombs were the unit of measurement for the total charge that passed through the concrete. For this test, the samples were cured for 28 days underwater. The chloride ion penetrability based on charge passed as per ASTM C1202 is shown in Table 6 and the experimental setup is shown in Fig. 10.

Table 6 Chloride ion penetration based on charge passed [56]

Chloride Penetration	RCPT Charged passed (Coulombs)
High	> 4000
Moderate	2000 to 4000
Low	1000 to 2000
Very Low	100 to 1000
Negligible	< 100

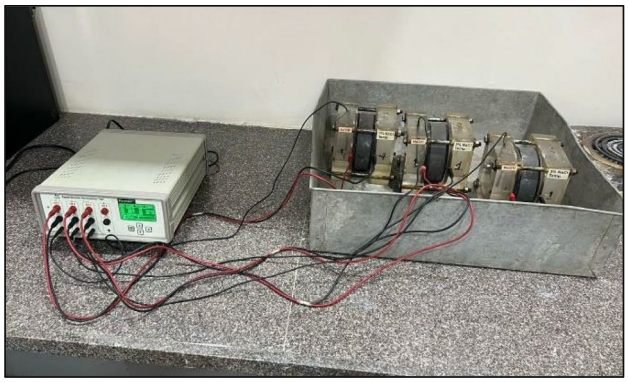

Fig. 10 Experimental setup for RCPT

Fig. 11 10% conc. HCl (acid attack test setup)

6.2.3 Acid attack test

The acid attack test was performed to check the durability and resistance of the concrete, and the 150 × 150 x 150 mm size cube samples were cast. As per ASTM C1898-20 [57], casted cube samples were first cured for 28 days underwater and then submerged in 10% concentrated HCl acid for another 28 days as

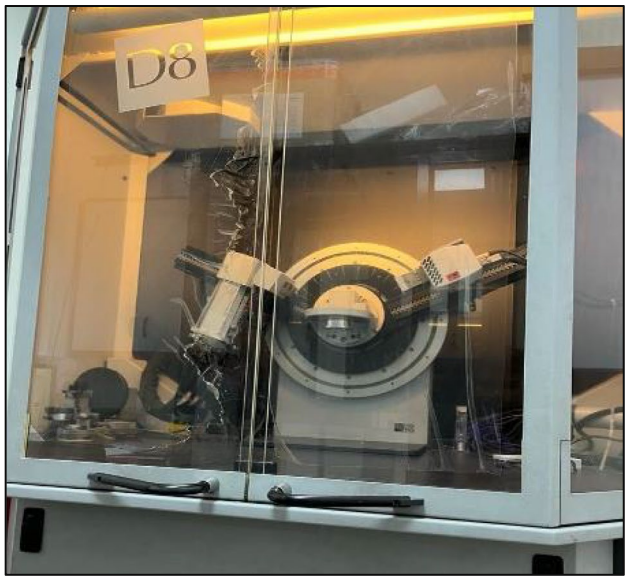

Fig. 12 X-ray diffractometer

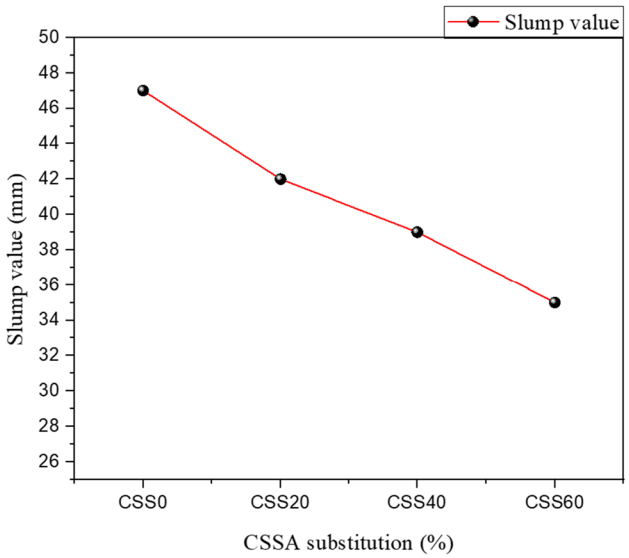

Fig. 13 Slump value

shown in Fig. 11 to check the weight difference before and after the acid attack. Acidic substances chemically react with the components of concrete, leading to various detrimental effects.

6.3 Microstructure analysis tests

6.3.1 X-ray diffraction analysis (XRD)

The X-ray diffractometer machine was used for the XRD analysis, as shown in Fig. 12. It is a non-destructive technique used to determine the crystallographic structure of material, chemical content, and physical attributes. In this experimental work, the XRD analysis was performed to compare the SSA and cement.

6.3.2 Scanning *electron* microscopy (SEM)

To check the microstructural bonding and composition of the concrete mixed with the CSSA, SEM analysis was performed after 28 days of the casting of samples, and microstructural images of the concrete bonding were captured. This analysis was focused on the changes observed in the microstructural characteristics, hydration products, and porosity of the CSSA particle mixed in the concrete.

7 Result and discussion

7.1 Workability

As per IS1199:1959 [51], the slump test was performed on fresh concrete. For the 0.4 w/c, the workability of the concrete mixed was observed, and due to voids, high water absorption capacity, and increasing substitution by CSSA results in less workability of the concrete mix as shown in Fig. 13. Also, the higher specific gravity of SSA relative to NCA is responsible for the decrease in the workability of concrete, for which the proper amount of superplasticizer content is to be added to increase the workability and the targeted strength [1, 58]. The desired slump of 25–50 mm was achieved by using 0.4% admixture with a 0.4 w/c ratio [59].

7.2 CS test result

A CS test was carried out on the concrete cube with the CSSA at 7, 14, and 28 days of the curing period. CS test results are shown in Fig. 14. An improvement in CS was observed because of the higher LA abrasion class of the CSSA as compared to the NCA. Also, CSSA has a rough texture, which improves the bonding with the cement (as shown in Fig. 15) and consequently the CS. Compared with the normal concrete sample (CSS0), substitution exhibited the highest strength for the sample CSS40, also compared with the CSS20 and CSS60. This is due to the Pozzolanic action which improves hydration and forms strong products that contribute to a hard concrete mix. Also, the increased density of concrete is responsible for CS improvement [60]. After 28 days of curing, the CS increased by 2.11% and 6.37% for mixtures with 20% and 40% substitution (CSS20 and CSS40), respectively. However, a decrease of 3.15% in CS was observed for the mixture with 60% substitution (CSS60). This decrease is likely due to the poorly shaped particles and differing chemical properties of CSSA, which weakens the bond between

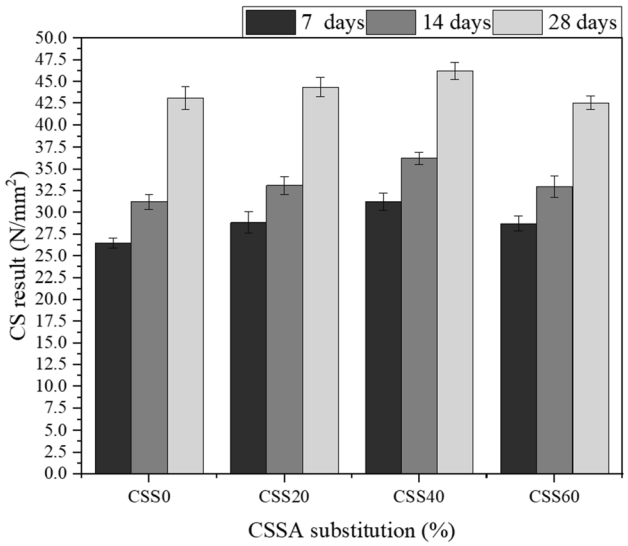

Fig. 14 CS test result

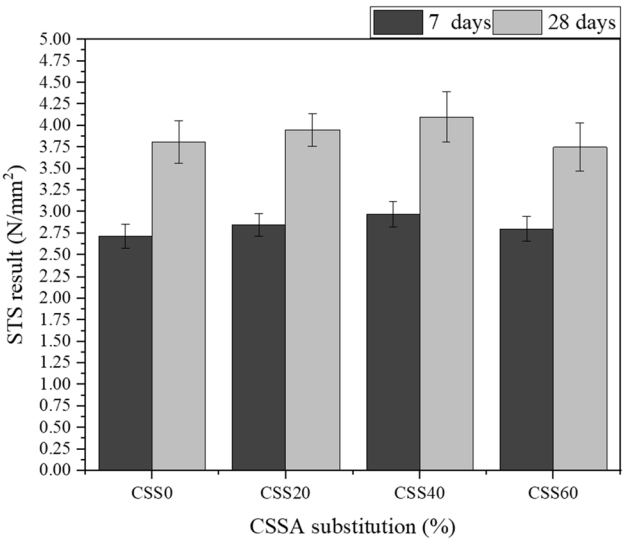

Fig. 16 STS test result

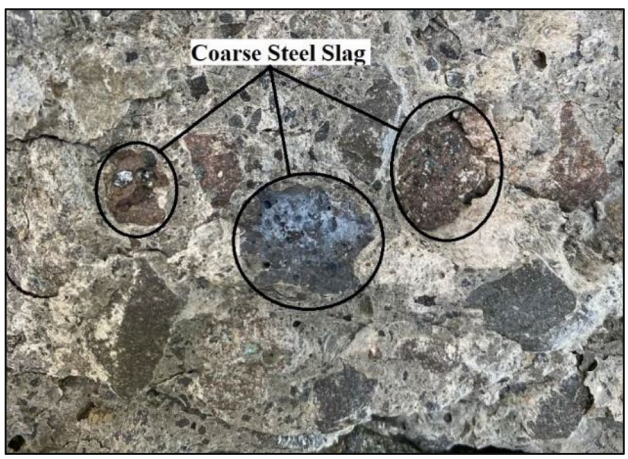

Fig. 15 CSSA bonding in concrete

particles and reduces overall strength. There was a negligible increase in CS by 0.98% and 2.33% for CSS20 and CSS40, respectively, and a decrease of 0.19% for CSS60 after 14 days of curing, and the same trend was followed at the 7 days of curing period, as shown in Fig. 14. The same observation was noticed by various researchers [3, 4, 45, 61, 62]. These results suggested that, up to a 40% amount of substitution, CSSA can be successfully substituted in concrete without sacrificing structural integrity.

7.3 STS test result

The STS test results at 7 and 28 days of the curing period are shown in Fig. 16. The experimental results state that the different percentages of CSSA substitution had a noticeable influence on the STS of the concrete samples CSS0, CSS20, CSS40, and CSS60. The highest STS was obtained for the sample of substitution of CSS40 by comparing it with CSS0 and also with CSS20 and CSS60. Beyond this threshold, the STS performance declined, suggesting an optimal balance between material substitution and mechanical properties. For the curing period of 7 days, the improvement in the STS of CSS20, CSS40, and CSS60 was noted at 5.14%, 9.19%, and 3.67%, respectively, compared with the CSS0. For the curing period of 28 days, the improvement in the STS for CSS20 and CSS40 was noted at 2.63% and 5.52%, respectively, and CSS60 was lower by 2.63%, as shown in Fig. 16. With an increase in CSSA content of more than 60% the STS is negatively impacted. Because of its not uniform size as an NCA, and it is not angular enough to allow for mechanical interlocking, the higher absorption of water impacts the w/c ratio, compromising the STS [63].

7.4 FS test result

The FS test performed on the beam and the result for 7 and 28 days of curing period are shown in Fig. 17. The highest FS resulted for the substitution sample of CSS40 after 28 days of curing, with an 8.40% strength improvement, as shown in Fig. 17. Comparing all the FS for the substitution with the CSS0, 4.49%, 9.63%, and 0.85% of strength improvement were achieved after 7 days of curing. For the 28-day curing period, 4.84%, 8.40%, and 2.03% of strength improvement were observed. Weaker interactions between CSSA and cement paste, rounded shapes of CSSA, stress-concentrating voids, and problems with water absorption are the factors that cause FS of the concrete to decrease beyond 40% substitution [7].

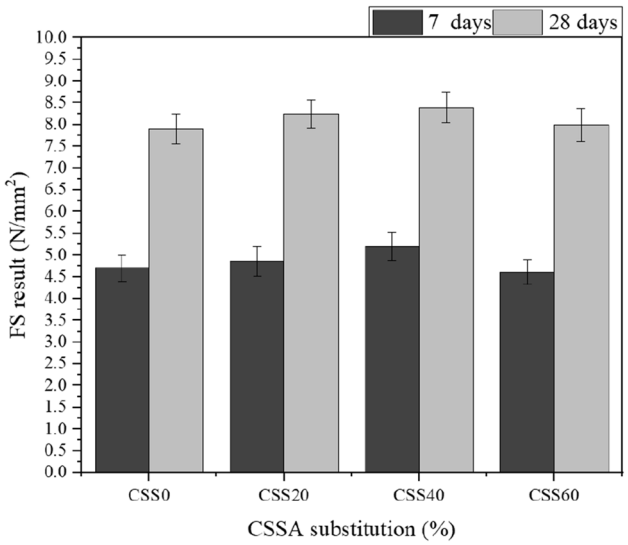

Fig. 17 FS test result

7.5 Relation between STS and CS result

The correlation between STS and CS test results of concrete with the substitution of CSSA is shown in Fig. 18, and the regression analysis findings were represented by Eqs. (2).

$$STS = 0.49107 + 0.07634 \times CS\left(\text{Coefficient of determination}, R^2 = 0.98773\right) \quad (2)$$

Equation (2) shows the strong, substantial linear relationship between the STS and CS after 28 days. The correlation coefficient was 0.98773. Because the coefficient of determination is close to 1, it represents a strong relationship between the STS and the CS for the substitution of CSSA for NCA.

7.6 Relation between FS and CS result

The correlation between FS and CS test results of concrete with the substitution of CSSA is shown in Fig. 19 and the regression analysis findings were represented by Eqs. (3).

$$FS = 3.96477 + 0.09417 \times CS\left(\text{Coefficient of determination}, R^2 = 0.76771\right) \quad (3)$$

Equation (3) exhibits a substantial polynomial relationship between the FS and CS for 28 days. The correlation coefficient was 0.76771. Because the coefficient of determination is close to 1, it indicates that a strong relationship exists between the FS and the CS for the substitution of CSSA for NCA.

7.7 Water penetration test

Following the German code DIN1048 [55], the coefficient of permeability is shown in Table 7. The water absorption capacity of the concrete depends on the volume, porousness, microstructural properties, and internal bonding between the materials. As the amount of CSSA increased, there was a decrease in water penetration depth. This suggests a denser material (low porosity) due to the inclusion of iron slag. These findings are confirmed and align with the CS and RCPT results.

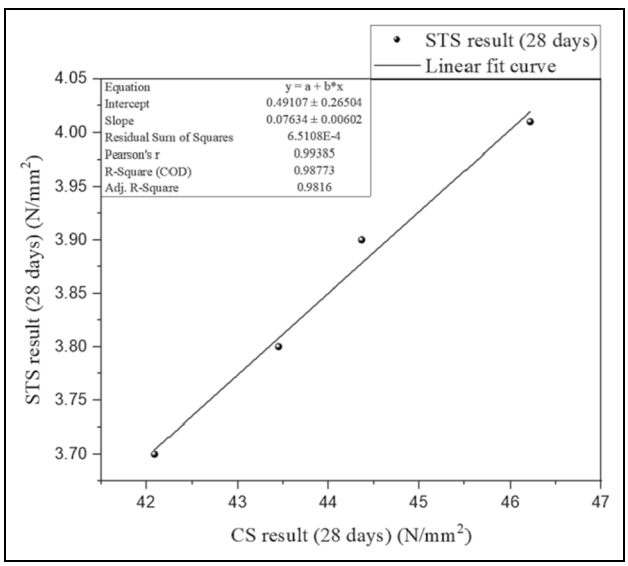

Fig. 18 Relation between STS vs CS test result

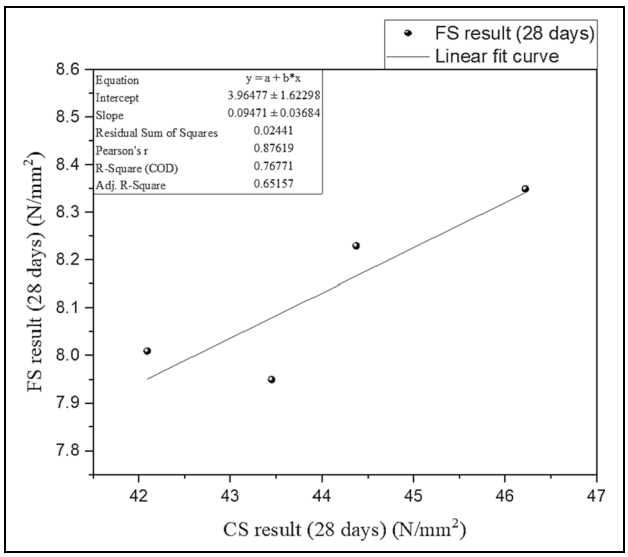

Fig. 19 Relation between FS and CS result

Table 7 Coefficient of permeability for CSSA substitution

Sample	CSS0	CSS20	CSS40	CSS60
Avg. Penetration Depth (mm)	19	15.8	11.5	15.5
Permeability $\times 10^{-10}$ (cm/sec)	6.823	4.716	2.499	5.563

Following a 72-h permeability test on 28-day cured concrete samples with CSSA, the observed decrease in the permeability coefficient appears to be correlated with an increasing trend of incorporating CSSA into concrete mixtures, as evidenced by the data presented in Table 7. Specifically, concrete samples labeled CSS0, CSS20, and CSS40, all exhibited a decreasing trend in penetration depth and a sudden increase in penetration depth due to an increase in the porous structure of CSSA and chemical composition. Due to the chemical composition and porous structure of CSSA, the coefficient of permeability of water is connected to its porosity [64, 65].

7.8 RCPT result

As per ASTM C1202 [56], the RCPT test was conducted on samples CSS0, CSS20, CSS40, and CSS60 and the experimented results are shown in * MERGEFORMAT Table 8. Replacing NCA with CSSA at any level significantly reduced permeability. Notably, the permeability decreased the most (40% reduction) at the 28-day curing mark with a 40% substitution ratio compared to other ratios. This decrease in permeability (measured by the amount of electrical charge passed) is likely due to a denser concrete matrix caused by the inclusion of CSSA. These findings are similar to the compressive strength results, where increased density from CSSA led to improved strength. This aligns with the results of Devi and Gnanavel [3], the observation that replacing 40% of fine aggregate with steel slag in conventional concrete enhances resistance to chloride ions. Low permeability values will be seen for the 20% and 40% substitution amounts of NCA with CSSA for the 28 days of curing and an increase in value will be observed when the substitution amount increases beyond 60%. The low permeability value up to 40% substitution level is due to a denser concrete produced by a CSSA content which improves CS also. The same observation was noticed by G. Singh and R. Siddique [66]. Up to a 20% substitution ratio of SSA in high-strength concrete, no significant impact on chloride ion permeability was observed. However, a considerable impact was noticed at a 30% substitution ratio [67].

7.9 Acid attack test result

As per ASTM C1898-20 [57], a loss in weight was observed in the sample cubes immersed in the 10% concentrated HCl acid, as shown in Fig. 11. In the test result, the concrete sample CSS0 got a weight loss of 0.41% compared to the samples CSS20, CSS40, and CSS60. It was seen that the CSSA has better acid resistance than the CSS0 by comparing the results as shown in Table 9. This is because the use of CSSA prevents the growth of calcium hydroxide around the NCA and FA particles, which improves the concrete's mechanisms for resistance to acid attack [26]. In the CS test, concrete sample CSS0 resulted in 3.58% strength loss, which is higher than the samples CSS20, CSS40, and CSS60 containing CSSA, as shown in Table 9.

7.10 SEM analysis test

The concrete containing CSSA was examined by SEM analysis as shown in Fig. 20. The image shows that the cement, water, and CSSA reaction creates a calcium silicate hydrate (C-S–H) gel. XRD analysis revealed characteristic peaks at 9.1°, 15.8°, and 22.9° 2θ, indicating the presence of ettringite in the sample. The quantified amount of ettringite was 2.5% by weight of cementitious material. This relatively low percentage is considered beneficial for early strength development and does not pose a threat to the integrity of concrete. Additionally, the presence of needle-like ettringite within the pores of the CSSA particles suggests cementitious properties of the CSSA, which was also supported by the chemical properties of CSSA as shown in Table 4, and quantitative analysis by XRD test as shown in Fig. 5. According to Fig. 21, CSSA particles were seen to be wrapped in the villus-like coating layer. The cracks between the CSSA particles and the surrounding cement paste were also observed with a width of approximately 0.62 µm. This crack width increases to about 1.57 µm between the NCA and the cement paste. Similar observations were reported by G. Wang et al. [68]. This resulted in the CSSA being porous and cementitious, which results in high water absorption and getting hydrated with CSSA, leading to a lower w/c ratio and a stronger interfacial transition zone (ITZ) between CSSA and cement paste [36].

The multi-angular shape and rough surface of CSSA particles contribute to a stronger ITZ between the particles and the cement paste. This effect is likely due to the increased contact area created by the villus-like structure coating on the CSSA particles.

Table 8 RCPT results

Sample	CSS0	CSS20	CSS40	CSS60
Density (KN/m^3)	23.50	23.80	24.20	23.70
Charged Passed (Coulombs)	1645	1560	1540	1550

Table 9 Acid attack test result

Sample	CSS0	CSS20	CSS40	CSS60
Loss in weight (%)	0.41	0.32	0.21	0.12
Loss in CS (%)	3.58	2.97	2.61	2.23

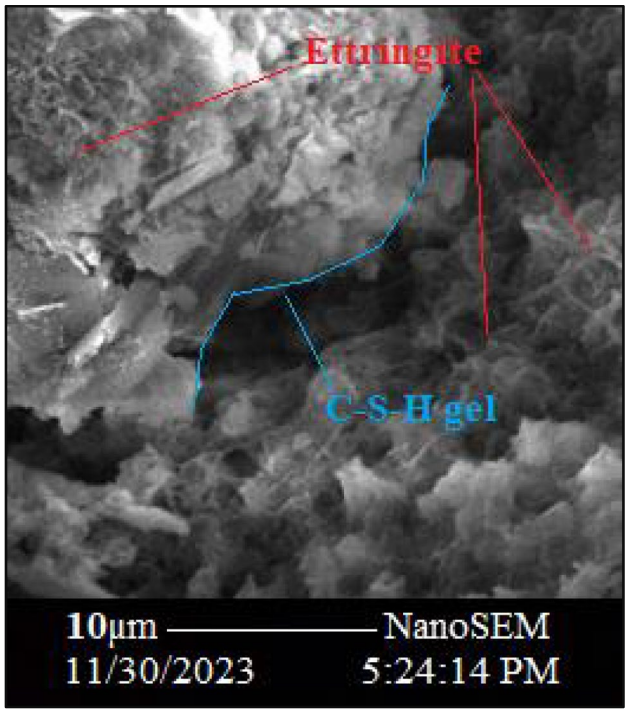

Fig. 20 Micro-morphology of CSSA particle in concrete

This enhanced interlocking improves the ITZ, as observed in Fig. 21. Similar observations were reported in [36, 68, 69]. A very smooth surface of NCA particles was noticed as the right half portion which was observed in Fig. 22.

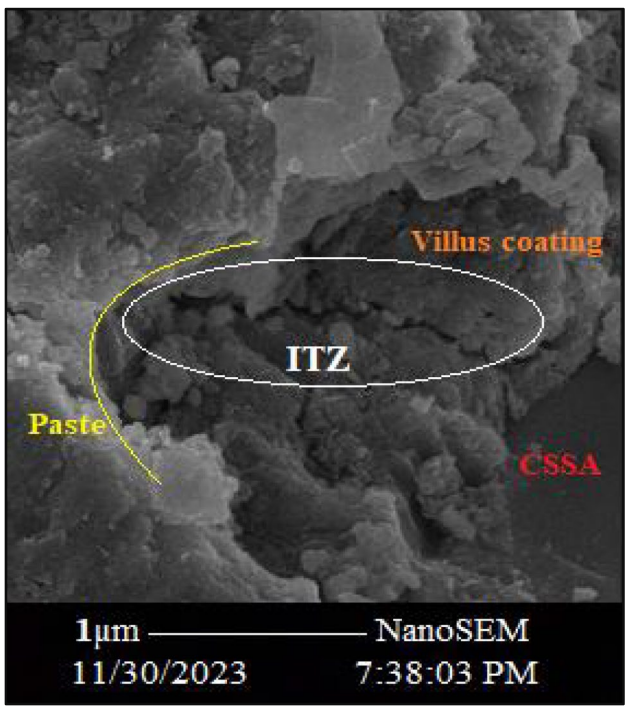

Fig. 21 ITZ of concrete with CSSA

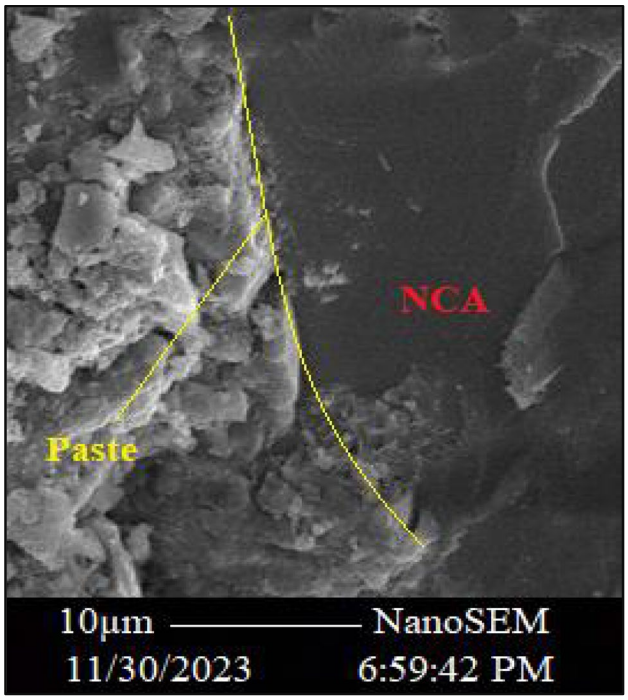

Fig. 22 ITZ of concrete without CSSA

8 Conclusion

The major conclusions derived from the present experimental study can be summarized as follows:

1) Experimental results showed that the optimum percentage of NCA substituted with CSSA was 40% in concrete led to improvements in CS and STS as well and the optimum percentage of NCA the substitution with CSSA was 20% for FS. Notably, the coefficient of determination being close to 1 indicates a strong correlation between both STS and CS, as well as FS and CS, when using CSSA as a substitute for NCA.
2) As the amount of CSSA increased, there was a decrease in water penetration depth up to 40% substitution level due to the formation of denser concrete with low porosity, and an increasing trend in penetration depth was observed at 60% substitution level due to the porous structure of CSSA and chemical composition. These findings are aligned with the CS and RCPT results.
3) The chloride ion permeability results show a decreasing trend up to 40% substitution level and increased at 60% which is similar to the trend observed in water penetration test results. This was measured by the amount of electrical charge passed through

the concrete sample and it was likely due to a denser concrete matrix caused by the inclusion of CSSA.

4) The concrete with CSSA shows good resistance to acid attack tests. The concrete sample was subjected to 10% of conc. HCl acid shows minimal effect on the concrete prepared with CSSA as compared to concrete with NCA. The response of the concrete against HCL acid was confirmed with CS and weight loss percentage results.
5) The XRD analysis for CSSA gets the sharp crystalline peaks at 2θ and contains cementitious chemical properties, i.e., C_3S and C_2S. Also, the analysis of the SEM result states that the CSSA could significantly improve the ITZ of concrete mix. Overall, utilizing CSSA as a substitute for NCA in concrete, with an appropriate substitutional ratio, gives significant benefits for sustainability and environmental impact reduction in construction materials. This contributes to enhancing both the mechanical, durability, and microstructural properties of concrete.

9 Future scopes

Future research should investigate optimizing the combined use of recycled coarse and fine aggregate (SSA) with various hybrid mineral admixtures in concrete. These hybrid admixtures could combine two or more materials like fly ash, metakaolin, rice husk ash, ground granulated blast furnace slag, or silica fume in different proportions. By partially replacing cement with these optimized combinations, the goal is to achieve sustainable concrete production through waste material utilization while enhancing concrete properties. Also, the study on chemical treatments to SSA to improve the durability of the concrete mix is an important aspect to improve its performance for the sustainable integration of SSA in the concrete industry.

Author contributions Saurabh Kalane: Conceptualization; Methodology, Investigation, Writing- original draft;
Shubhangi Shekokar: Supervision, Review.
Sandeep Sathe: Supervision, Review.
Rohit Salgude: Supervision, Review.

Funding The authors have not disclosed any funding.

Data availability No datasets were generated or analysed during the current study.

Declarations

Competing interests The authors declare no competing interests.

References

1. Faleschini F, Alejandro Fernández-Ruíz M, Zanini MA, Brunelli K, Pellegrino C, Hernández-Montes E (2015) High performance concrete with electric arc furnace slag as aggregate: Mechanical and durability properties. Constr Build Mater 101:113–121. https://doi.org/10.1016/j.conbuildmat.2015.10.022
2. Han XYJOB (2014) Self-sensing concrete in smart structures. Elsevier. https://doi.org/10.1016/C2013-0-14456-X
3. Subathra Devi V, Gnanavel BK (2014) Properties of concrete manufactured using steel slag. In: Procedia Eng, Elsevier Ltd, pp 95–104. https://doi.org/10.1016/j.proeng.2014.12.229
4. Vijayaraghavan J, Jude AB, Thivya J (2017) Effect of copper slag, iron slag and recycled concrete aggregate on the mechanical properties of concrete. Resour Policy 53:219–225. https://doi.org/10.1016/j.resourpol.2017.06.012
5. Ouda AS, Abdel-Gawwad HA (2017) The effect of replacing sand by iron slag on physical, mechanical and radiological properties of cement mortar. HBRC J 13:255–261. https://doi.org/10.1016/j.hbrcj.2015.06.005
6. Coppola L, Buoso A, Coffetti D, Kara P, Lorenzi S (2016) Electric arc furnace granulated slag for sustainable concrete. Constr Build Mater 123:115–119. https://doi.org/10.1016/j.conbuildmat.2016.06.142
7. Santamaría A, Romera JM, Marcos I, Revilla-Cuesta V, Ortega-López V (2022) Shear strength assessment of reinforced concrete components containing EAF steel slag aggregates. J Build Eng 46:103730. https://doi.org/10.1016/j.jobe.2021.103730
8. Wagale M, Dandin S, Bokil S, Sathe S (2023) Potential use of fly ash in structural fill application: a review. Environ Sci Pollut Res. https://doi.org/10.1007/s11356-023-30968-w
9. Sathe S, Patil V (2021) An experimentation on properties of geo-polymer concrete with fibres. Turk J Comput and Math Educ (TURCOMAT). https://doi.org/10.17762/turcomat.v12i13.8233
10. Dhalape P, Sathe S, Dekhane C (2022) An experimental study on cement concrete with industrial fly ash and Phosphogypsum. Mater Today Proc. https://doi.org/10.1016/j.matpr.2022.11.365
11. Sathe S, Zain Kangda M, Dandin S (2022) An experimental study on rice husk ash concrete. Mater Today Proc. https://doi.org/10.1016/j.matpr.2022.11.366
12. Dandin S, Kulkarni M, Wagale M, Sathe S (2022) A review on the geotechnical response of fly ash-colliery spoil blend and stability of coal mine dump. Clean Waste Syst 3:100040. https://doi.org/10.1016/j.clwas.2022.100040
13. Sathe S, Patil S (2023) Experimental analysis and behavior of corrosion-damaged fly ash blended reinforced concrete beam under flexural loading. J Build Pathol Rehab 8:97. https://doi.org/10.1007/s41024-023-00344-9
14. Sathe S, Patil S, Bhosale A (2023) Effectiveness of fly ash as corrosion inhibitor for reinforced concrete beam under torsion. Innov Infrastruct Solutions 8:275. https://doi.org/10.1007/s41062-023-01246-y
15. Sathe S, Patil S, Shete V (2023) An experimental study on flexural strength of corroded-reinforced concrete beam with fly ash. In: lecture notes in civil engineering. Springer science and business media Deutschland GmbH, pp 87–96. https://doi.org/10.1007/978-981-19-4055-2_8
16. Baalamurugan J, Kumar VG, Chandrasekaran S, Balasundar S, Venkatraman B, Padmapriya R, Raja VKB (2021) Recycling of steel slag aggregates for the development of high density concrete: alternative & environment-friendly radiation shielding composite. Compos B Eng 216:108885. https://doi.org/10.1016/j.compositesb.2021.108885

17. Rosales J, Cabrera M, Agrela F (2017) Effect of stainless steel slag waste as a replacement for cement in mortars. Mech Stat Study Constr Build Mater 142:444–458. https://doi.org/10.1016/j.conbuildmat.2017.03.082
18. Evangelista BL, Rosado LP, Penteado CSG (2018) Life cycle assessment of concrete paving blocks using electric arc furnace slag as natural coarse aggregate substitute. J Clean Prod 178:176–185. https://doi.org/10.1016/j.jclepro.2018.01.007
19. Singh N, Singh A, Ankur N, Kumar P, Kumar M, Singh T (2022) Reviewing the properties of recycled concrete aggregates and iron slag in concrete. J Build Eng 60:105150. https://doi.org/10.1016/j.jobe.2022.105150
20. Anastasiou EK, Liapis A, Papachristoforou M (2017) Life cycle assessment of concrete products for special applications containing EAF slag, procedia. Environ Sci 38:469–476. https://doi.org/10.1016/j.proenv.2017.03.138
21. Zareei SA, Ameri F, Bahrami N, Shoaei P, Moosaei HR, Salemi N (2019) Performance of sustainable high strength concrete with basic oxygen steel-making (BOS)slag and nano-silica. J Build Eng 25:100791. https://doi.org/10.1016/j.jobe.2019.100791
22. Maslehuddin M, Sharif AM, Shameem M, Ibrahim M, Barry M (2003) Comparison of properties of steel slag and crushed limestone aggregate concretes. Construct Build Mater 17(2):105–112. https://doi.org/10.1016/S0950-0618(02)00095-8
23. Yang S, Mo L, Deng M (2021) Effects of ethylenediamine tetraacetic acid (EDTA) on the accelerated carbonation and properties of artificial steel slag aggregates. Cem Concr Compos 118:103948. https://doi.org/10.1016/j.cemconcomp.2021.103948
24. Pan SY, Adhikari R, Chen YH, Li P, Chiang PC (2016) Integrated and innovative steel slag utilization for iron reclamation, green material production and CO2 fixation via accelerated carbonation. J Clean Prod 137:617–631. https://doi.org/10.1016/j.jclepro.2016.07.112
25. Palankar N, Ravi Shankar AU, Mithun BM (2016) Durability studies on eco-friendly concrete mixes incorporating steel slag as coarse aggregates. J Clean Prod 129:437–448. https://doi.org/10.1016/j.jclepro.2016.04.033
26. Venkatesan B, Lijina VJ, Kannan V, Dhevasenaa PR (2020) Partial replacement of fine aggregate by steel slag and coarse aggregate by walnut shell in concrete. In: Mater Today Proc, Elsevier Ltd, pp 1761–1766. https://doi.org/10.1016/j.matpr.2020.07.361
27 Sekaran A, Palaniswamy M, Balaraju S (2015) A study on suitability of EAF oxidizing slag in concrete: an eco-friendly and sustainable replacement for natural coarse aggregate. Sci World J 2015:1. https://doi.org/10.1155/2015/972567
28 Gencel O, Karadag O, Oren OH, Bilir T (2021) Steel slag and its applications in cement and concrete technology: a review. Constr Build Mater 283:122783. https://doi.org/10.1016/j.conbuildmat.2021.122783
29. Van Tran M, Van Nguyen C, Nawa T, Stitmannaithum B (2015) Properties of high strength concrete using steel slag coarse aggregate. ASEAN Eng J 4(2):22–32. https://doi.org/10.11113/aej.v4.15448
30. Miah MJ, Miah MS, Sultana A, Shamim TA, Alom MA (2020) The effect of steel slag coarse aggregate on the mechanical and durability performances of concrete. In: Key Eng Mater, Trans Tech Publications Ltd, pp 228–232. https://doi.org/10.4028/www.scientific.net/KEM.833.228
31. Malathy R, Arivoli M, Chung IM, Prabakaran M (2021) Effect of surface-treated energy optimized furnace steel slag as coarse aggregate in the performance of concrete under corrosive environment. Constr Build Mater 284:122840. https://doi.org/10.1016/j.conbuildmat.2021.122840
32. Arribas I, Vegas I, San-José JT, Manso JM (2014) Durability studies on steelmaking slag concretes. Mater Des 63:168–176. https://doi.org/10.1016/j.matdes.2014.06.002
33. Biskri Y, Achoura D, Chelghoum N, Mouret M (2017) Mechanical and durability characteristics of high performance concrete containing steel slag and crystalized slag as aggregates. Constr Build Mater 150:167–178. https://doi.org/10.1016/j.conbuildmat.2017.05.083
34. Adegoloye G, Beaucour AL, Ortola S, Noumowé A (2015) Concretes made of EAF slag and AOD slag aggregates from stainless steel process: mechanical properties and durability. Constr Build Mater 76:313–321. https://doi.org/10.1016/j.conbuildmat.2014.12.007
35. Qasrawi H (2018) Fresh properties of green SCC made with recycled steel slag coarse aggregate under normal and hot weather. J Clean Prod 204:980–991. https://doi.org/10.1016/j.jclepro.2018.09.075
36. Lai MH, Zou J, Yao B, Ho JCM, Zhuang X, Wang Q (2021) Improving mechanical behavior and microstructure of concrete by using BOF steel slag aggregate. Constr Build Mater 277:122269. https://doi.org/10.1016/j.conbuildmat.2021.122269
37. Indian Standards IS 4031–1 (1996) Methods of physical tests for hydraulic cement, Part 1: determination of fineness by dry sieving, Bureau of Indian Standards, New Delhi, India
38. Indian Standards IS 12269 (2013) 53 grade ordinary Portland cement, Bureau of Indian Standards, New Delhi, India
39. Indian Standards (2016) IS383–2016 coarse and fine aggregate for concrete - specification (third revision), Bureau of Indian Standards, New Delhi, India
40. Indian Standards IS 2720–3–1 (1980) Methods of test for soils, Part 3: determination of specific gravity, section 1: fine grained soils, Bureau of Indian Standards, New Delhi, India
41. Indian Standards IS 2386–3 (1963) Methods of test for aggregates for concrete, Part 3: specific gravity, density, voids, absorption and bulking, Bureau of Indian Standards, New Delhi, India
42. Indian Standards IS 2386–4 (1963) Methods of test for aggregates for concrete, Part 4: mechanical properties, Bureau of Indian Standards, New Delhi, India
43. Indian Standards IS 2386–5 (1963): methods of test for aggregates for concrete, Part V: soundness [CED 2: cement and concrete], Bureau of Indian Standards, New Delhi, India
44. Lai MH, Chen MT, Ren FM, Ho JCM (2019) Uni-axial behaviour of externally confined UHSCFST columns. Thin-Walled Struct 142:19–36. https://doi.org/10.1016/j.tws.2019.04.047
45. Qiang W, Mengxiao S, Jun Y (2016) Influence of classified steel slag with particle sizes smaller than 20 μm on the properties of cement and concrete. Constr Build Mater 123:601–610. https://doi.org/10.1016/j.conbuildmat.2016.07.042
46. Zhang Z, Hao Z, Gao Z (2015) A dynamic adjustment and distribution method of air traffic flow en-route. J Air Transp Manag 42:15–20. https://doi.org/10.1016/j.jairtraman.2014.07.007
47. Chen MT, Young B, Martins AD, Camotim D, Dinis PB (2020) Experimental investigation on cold-formed steel stiffened lipped channel columns undergoing local-distortional interaction. Thin-Walled Struct 150:106682. https://doi.org/10.1016/j.tws.2020.106682
48. Chen MT, Young B (2020) Beam-column tests of cold-formed steel elliptical hollow sections. Eng Struct 210:109911. https://doi.org/10.1016/j.engstruct.2019.109911
49 Lai M, Li C, Ho JCM, Chen MT (2020) Experimental investigation on hollow-steel-tube columns with external confinements. J Constr Steel Res 166:105865. https://doi.org/10.1016/j.jcsr.2019.105865
50. Indian Standards IS 10262 (2019) Guidelines for concrete mix design proportioning, Bureau of Indian Standards, New Delhi, India
51. Indian Standards IS 1199 (1959) Methods of sampling and analysis of concrete, Bureau of Indian Standards, New Delhi, India
52. Indian Standards IS 10086 (1982) Specification for moulds for use in tests of cement and concrete, Bureau of Indian Standards, New Delhi, India

53. Indian Standards IS 516 (1959) Methods of tests for strength of concrete cement, concrete sectional committee, Bureau of Indian Standards, New Delhi, India
54. Indian Standards IS 5816 (1999) Method of test splitting tensile strength of concrete, Bureau of Indian Standards, New Delhi, India
55. DIN1048 Standards (1991) DIN 1048 (Part 5): Testing concrete: testing of hardened concrete specimens prepared in mould, German Institute for Standardization, Germany.
56. ASTM Standards (2012) ASTM C1202: standard test method for electrical indication of concrete's ability to resist chloride ion penetration 1. https://doi.org/10.1520/C1202-12
57. ASTM (n.d.) ASTM C1898–20: standard test methods for determining the chemical resistance of concrete products to acid attack 1. https://doi.org/10.1520/D1898-20
58. Brand AS, Roesler JR (2015) Steel furnace slag aggregate expansion and hardened concrete properties. Cem Concr Compos 60:1–9. https://doi.org/10.1016/j.cemconcomp.2015.04.006
59. Palankar N, Ravi Shankar AU, Mithun BM (2017) Investigations on alkali-activated slag/fly ash concrete with steel slag coarse aggregate for pavement structures. Int J Pavement Eng 18:500–512. https://doi.org/10.1080/10298436.2015.1095902
60. Baalamurugan J, Ganesh Kumar V, Chandrasekaran S, Balasundar S, Venkatraman B, Padmapriya R, Bupesh Raja VK (2019) Utilization of induction furnace steel slag in concrete as coarse aggregate for gamma radiation shielding. J Hazard Mater 369:561–568. https://doi.org/10.1016/j.jhazmat.2019.02.064
61. Majhi RK, Nayak AN, Mukharjee BB (2018) Development of sustainable concrete using recycled coarse aggregate and ground granulated blast furnace slag. Constr Build Mater 159:417–430. https://doi.org/10.1016/j.conbuildmat.2017.10.118
62. Kothei L, Malathy R (2012) Mechanical properties of self-compacting concrete with partial replacement of natural sand by steel slag. Int J Earth Sci Eng 5(03):01
63. Abd El-Hakim RT, Elgendy GM, El-Badawy SM, Amin M (2022) Performance evaluation of steel slag high performance concrete for sustainable pavements. Int J Pavement Eng 23:3819–3837. https://doi.org/10.1080/10298436.2021.1922908
64. Öz HÖ (2018) Properties of pervious concretes partially incorporating acidic pumice as coarse aggregate. Constr Build Mater 166:601–609. https://doi.org/10.1016/j.conbuildmat.2018.02.010
65. Zaetang Y, Sata V, Wongsa A, Chindaprasirt P (2016) Properties of pervious concrete containing recycled concrete block aggregate and recycled concrete aggregate. Constr Build Mater 111:15–21. https://doi.org/10.1016/j.conbuildmat.2016.02.060
66. Singh G, Siddique R (2016) Effect of iron slag as partial replacement of fine aggregates on the durability characteristics of self-compacting concrete. Constr Build Mater 128:88–95. https://doi.org/10.1016/j.conbuildmat.2016.10.074
67. Wang Q, Wang D, Zhuang S (2017) The soundness of steel slag with different free CaO and MgO contents. Constr Build Mater 151:138–146. https://doi.org/10.1016/j.conbuildmat.2017.06.077
68. Wang G, Chen X, Dong Q, Yuan J, Hong Q (2020) Mechanical performance study of pervious concrete using steel slag aggregate through laboratory tests and numerical simulation. J Clean Prod 262:121208. https://doi.org/10.1016/j.jclepro.2020.121208
69. Chen X, Wang G, Dong Q, Zhao X, Wang Y (2020) Microscopic characterizations of pervious concrete using recycled steel slag aggregate. J Clean Prod 254:120149. https://doi.org/10.1016/j.jclepro.2020.120149